Supplementary Figures

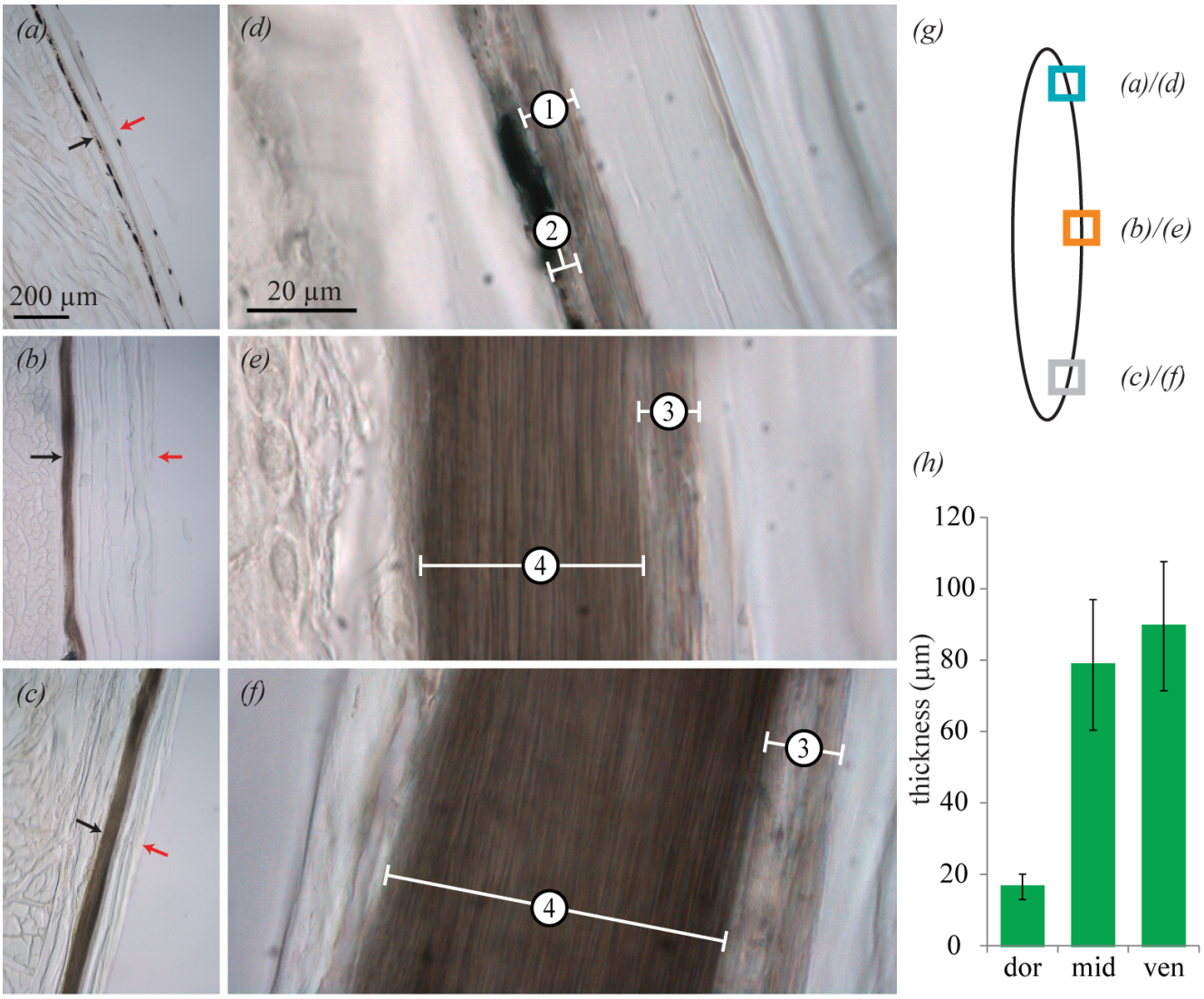

Fig. S1. Thicknesses of iridophore layers in different regions of the lookdown skin. *(a-f)* Images of cross sections of the skin from the dorsolateral *(a, d)*, mid-lateral *(b, e)*, and ventrolateral *(c, f)* flanks with transmitted illumination. *(a)*, *(b)* and *(c)* are low-magnification images and *(d)*, *(e)* and *(f)* are high-magnification images. *(g)* is a schematic outline of the fish cross section (black line). The blue, orange and gray squares indicate the locations of the dorsolateral *(a, d)* , mid-lateral *(b, e)*, and ventrolateral *(c, f)* sections, respectively. Red arrows in *(a-c)* point to the surface of the fish and the black arrows point to the iridophore layer (stratum argenteum). The white bars demarcate the layers of Type 1 and Type 2 guanine platelets in *(d)*, Type 3 and Type 4 in *(e, f)*. *(h)* shows the total thicknesses of iridophore layers. One-way ANOVA indicates that these layers are significantly different in thickness ($F=2043$, $p < 0.001$). Tukey-Kramer post hoc tests (with 0.01 error rate) shows that the iridophore layer in the dorsolateral flank is significantly thinner than those in the mid-lateral and ventrolateral regions, and that the iridophore layer in the mid-lateral flank is also significantly thinner than that in the ventrolateral skin. The arrow bars in *(h)* represent the standard deviations.

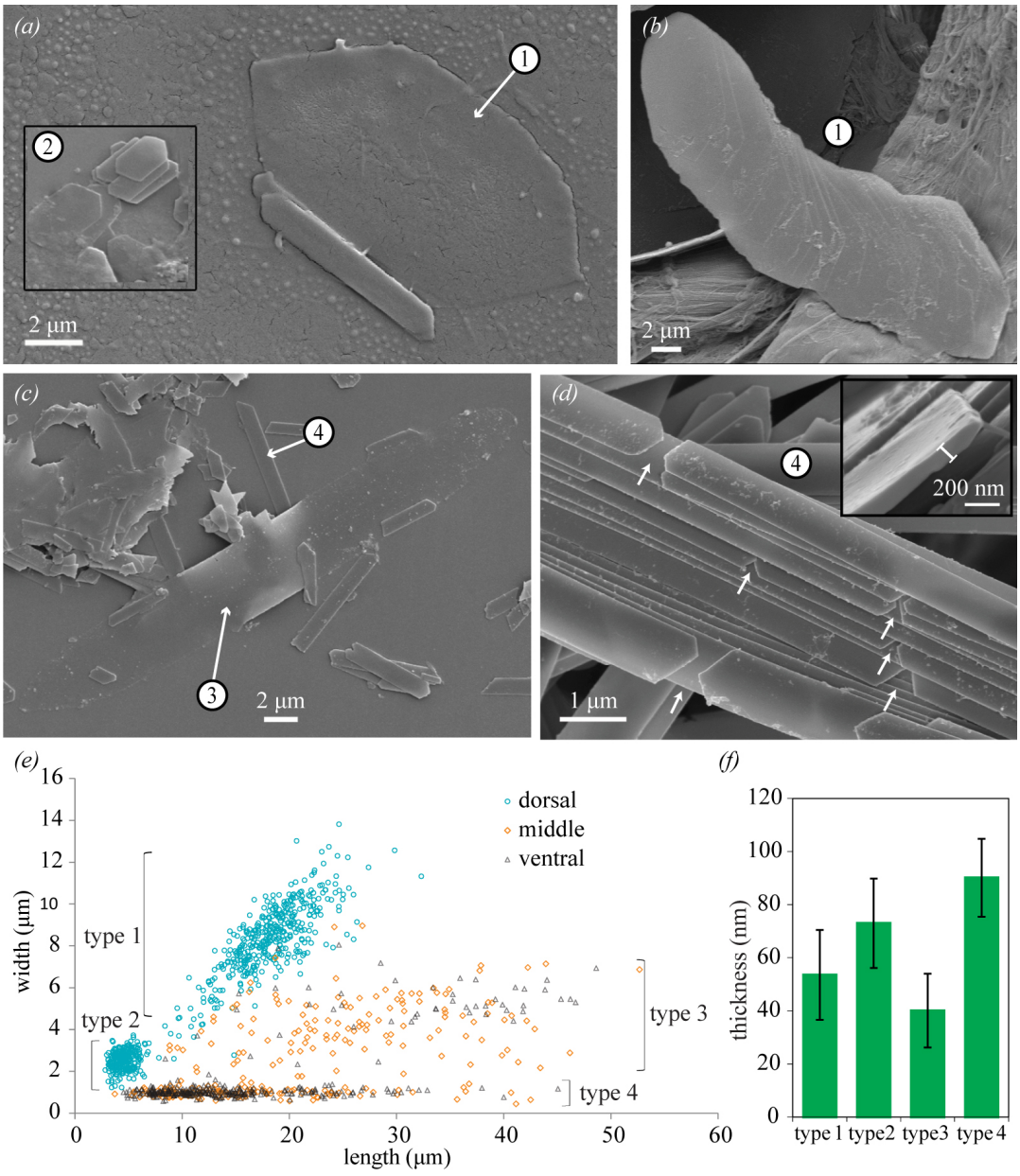

Fig. S2. Dissociated guanine platelets and their dimensions. SEM images of dissociated guanine platelets from the dorsolateral *(a, b)* and mid-lateral flanks *(c, d)*. *(a)* The Type 1 platelet is much larger than the Type 2 platelet (the inlet) in the dorsolateral flank. *(b)* A stack of Type 1 platelets. *(c)* The Type 3 platelet is much wider than the Type 4 platelet in the mid-lateral flank. *(d)* A stack of Type 4 guanine platelets exhibit multiple gaps between individual guanine platelets (arrows). The inlet in *(d)* is a side-view of a Type 4 guanine platelet. High magnification images like this were used to estimate the thickness of individual guanine platelets (the white bar). *(e)* Dimensions of individual guanine platelets from dorsolateral (blue), mid-lateral (orange), and ventrolateral (gray) flanks. The distribution of Types 1-4 platelets are indicated by the brackets. *(f)* Average thicknesses of Types 1, 2, 3 and 4 guanine platelets are 53.5 ± 16.9 nm, 73.0 ± 16.8 nm, 40.1 ± 13.9 nm, and 90.1 ± 14.6 nm (mean ± SD), respectively. One-way ANOVA indicates significant differences among the thicknesses of different types of platelets ($F=177.6$, $p < 0.001$). Dukey-Kramer post hoc tests show that each type of the platelets is different from another type in thickness. The error bars in *(f)* represent the standard deviations.

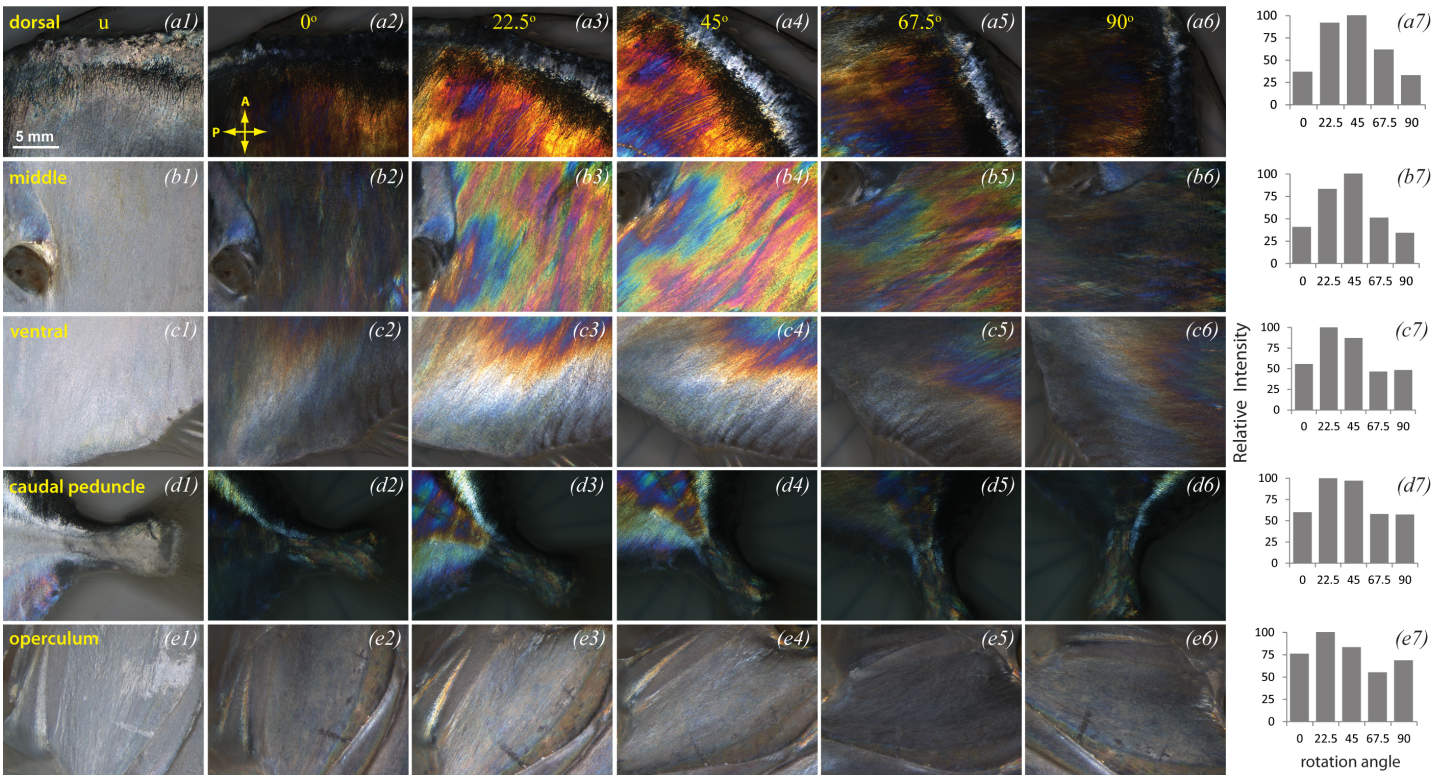

Fig. S3. Birefringence effects of the juvenile lookdown surface visualized by cross-polarization microscopy. The anterior-posterior axis of the fish is horizontal with the fish head on the left. The areas analyzed include dorsal *(a1-a7)*, middle *(b1-b7)* and ventral *(c1-c7)* flanks, the caudal peduncle *(d1-d7)* and the operculum *(e1-e7). (a1)-(e1)* are images taken with unpolarized light (u). *(a2)-(e2)* are images of the same views taken with crossed polarizers. The next four columns of images were taken with crossed polarizers after the fish was rotated from its natural swimming position (0^o) clockwise by 22.5, and 45, 67.5, or 90 degrees, respectively. The orientations of the polarizer (p) and analyzer (a) are indicated by the arrows in *(a2).* The normalized average intensities of cross-polarization images for different rotation angles are shown in *(a7)-(e7).* Note that for the dorsolateral and mid-lateral flanks, the maximum intensity was observed when the fish was rotated by 45^o while for ventralateral skin, the caudal peduncle, and the operculum, the maximum was reached at 22.5^o.

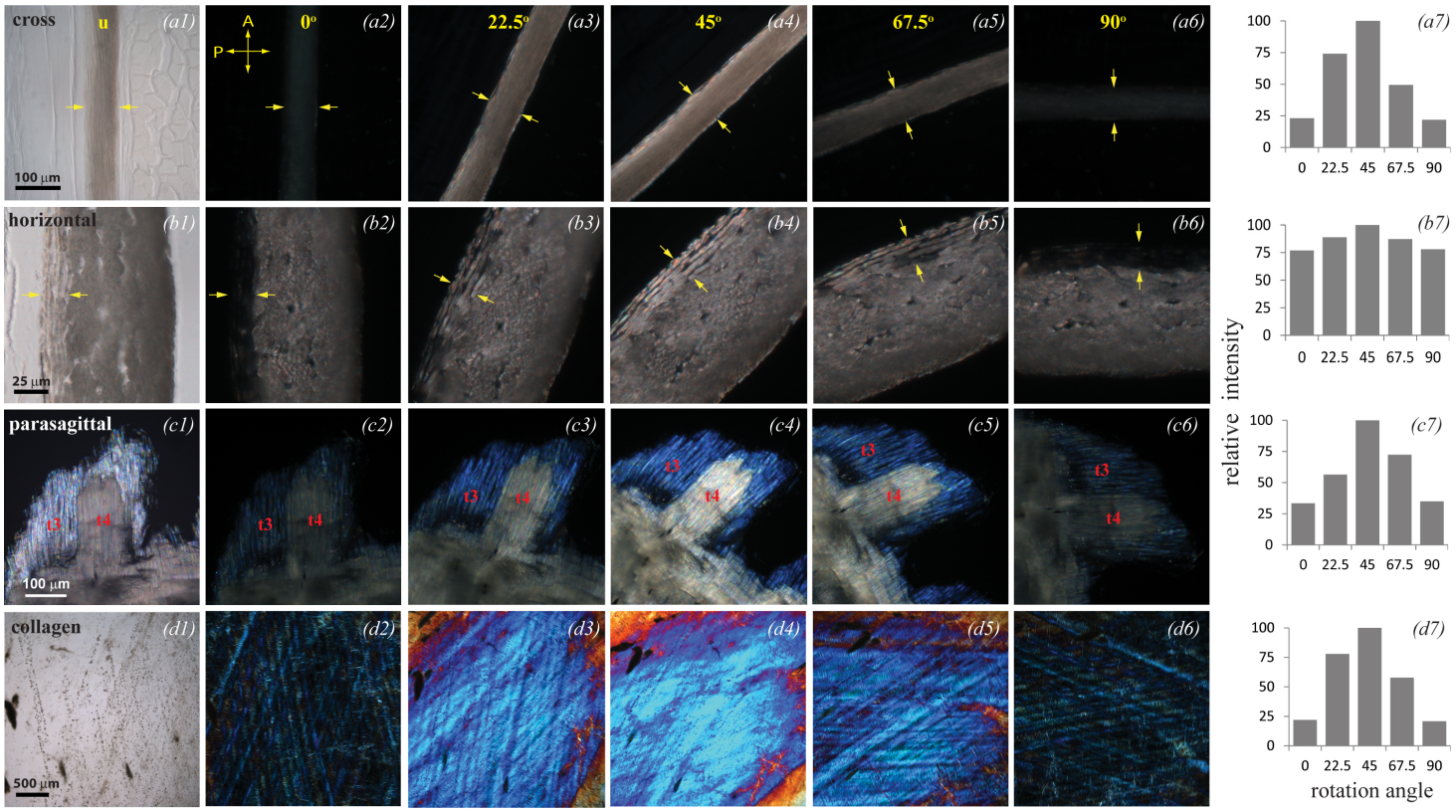

Fig. S4. Birefringence effects of the iridophore layer from the mid-lateral flank in cross *(a1-a7)*, horizontal *(b1-b7)* and parasagittal *(c1-c7)* sections and birefringence effects of the collagen layer *(d1-d7)*. All images were taken with transmitted illumination except those in (*c1-c6*) that were taken with epi-illumination. The first column *(a1-d1),* are images taken without polarizers. The next five columns of images were taken with crossed polarizers as the samples were rotated clockwise by 0, 22.5, and 45, 67.5, and 90 degrees, respectively. The orientations of the polarizer (p) and analyzer (a) are indicated by the arrows in *(a2). (a2-a6)* The arrows mark the iridophore layer. Minimum amount of light passed through the analyzer when the iridophore layer was vertical (0^{o}) or horizontal (90^{o}). Maximum amount of light passed through when the layer was rotated by 45^{o}. *(b2-b6)* The arrows indicate the layer of Type 3 guanine platelets. The visibility of Type 3 platelets changed from nearly zero to maximum as the section was rotated from 0 to 45^{o}. Thereafter, it decreased and became nearly invisible again at 90^{o}. In contrast, the visibility of Type 4 guanine platelets changed very little as the section was rotated from 0^{o} to 90^{o}. *(c2-c6)* In the parasagittal section, the long axes of Type 3 (t3) and Type 4 (t4) were in the same orientation. They both had minimum visibility when their long axes were in vertical or horizontal position while the maximum visibility was reached as the section was rotated by 45^{o}. The Type 3 platelets appeared blue while Type 4 platelets were multi-colored at high magnification and appeared nearly white at low magnification. *(d2-d6)* The collagen layer showed minimum visibility when it was in its natural orientation *(d2)* or rotated by 90^{o} *(d6).* Its intensity reached the maximum when rotated by 45^{o}. The last column, *(a7-d7),* shows the normalized average intensities of cross-polarization images of the iridophore and collagen layers.

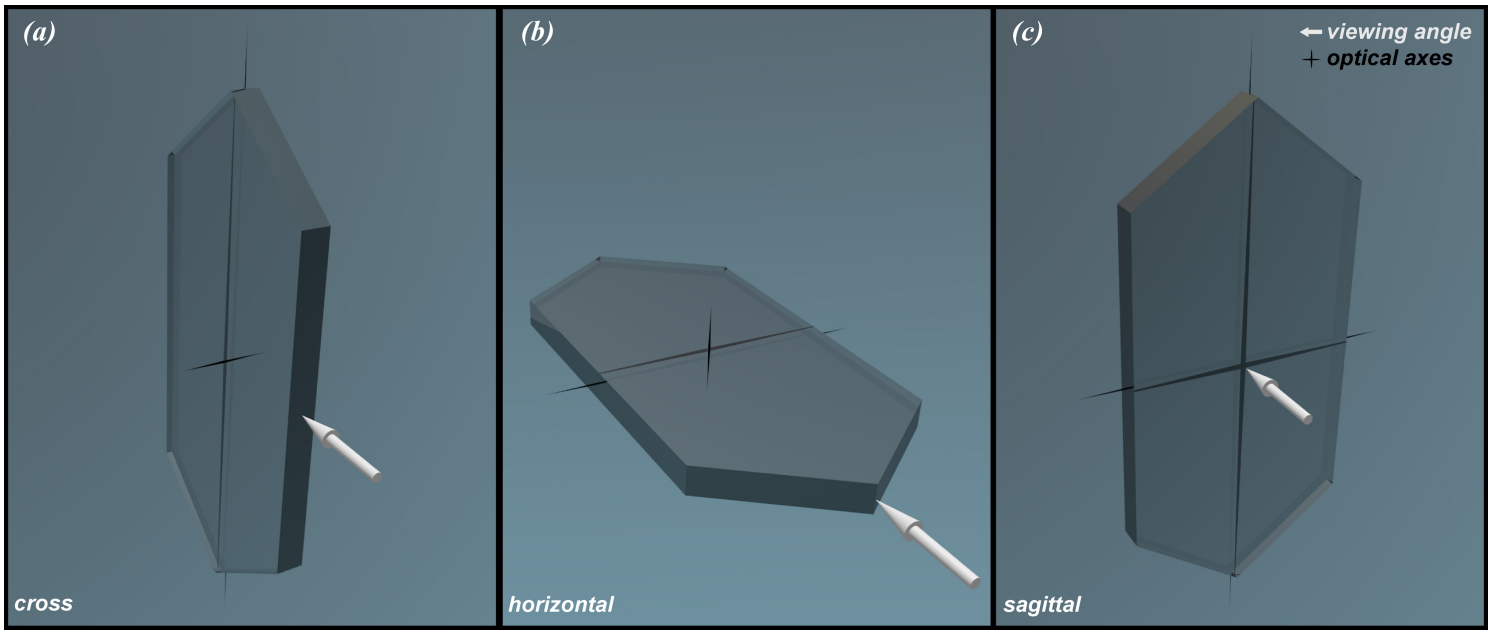

Fig. S5. Possible optical axes of the guanine platelets. The viewing direction is indicated by the white arrow and the possible optical axes by the black lines. *(a)* Results from cross sections shown in Fig. S4*a1-a7* indicate that at least a subset of the guanine platelets have their optical axes along the long axis and/or perpendicular to the reflecting surface. *(b)* Results from horizontal sections shown in Fig. S4*b1-b7* indicate that at least a subset of the guanine platelets have their optical axes along the short axis and/or perpendicular to the reflecting surface. *(c)* Data from the parasagittal sections shown in Fig. S4*c1-c7* indicate that at least a sub-population of Types 3 and 4 guanine platelets have their optical axes along the long axis and/or the short axis of the platelets.

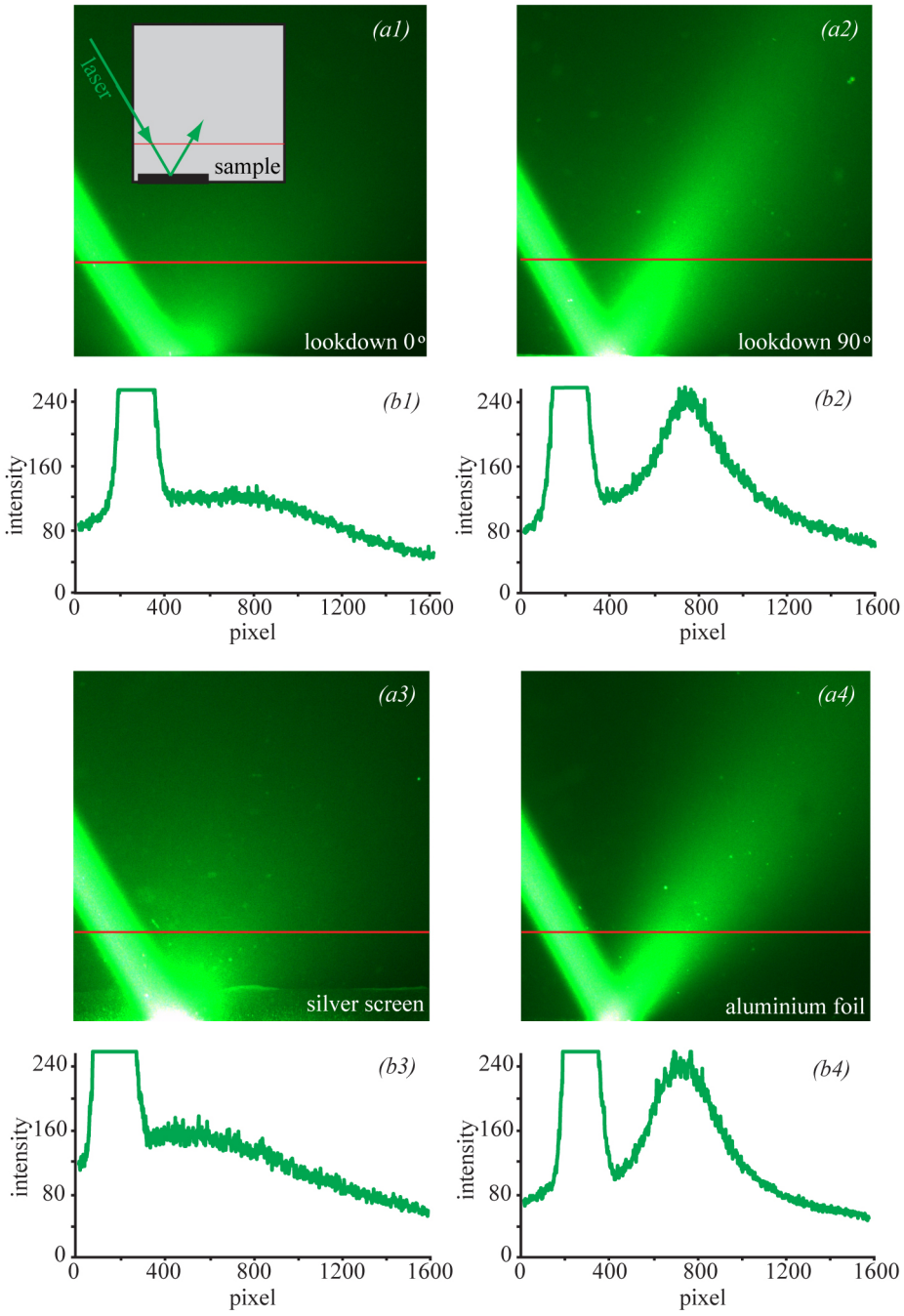

Fig. S6. Reflectance distribution of a laser beam from the lookdown skin. *(a1)* The inlet shows the setup for evaluating reflectance distribution of a laser beam from a sample surface. The sample was placed against one side of a plastic box containing low concentration of milk dissolved in PBS. A laser beam was directed to the sample through a glass window. When the lookdown skin was oriented as in a natural swimming position (the anterior-posterior axis of the fish was parallel to the water surface), the laser beam was scattered diffusely. *(a2)* When the skin was turned 90^{o}, a strong component of specular reflection was seen. *(a3)* The laser beam was diffusely scattered from a silver screen. *(a4)* In contrast, a significant specular component was reflected from the aluminum foil. *(b1-b4)* are intensity profiles at the red lines for *(a1-a4)*, respectively.